Journal of Materials Chemistry C

PAPER

View Article Online
View Journal | View Issue

Cite this: J. Mater. Chem. C, 2016, 4, 6894

Resolving the source of blue luminescence from alkyl-capped silicon nanoparticles synthesized by laser pulse ablation†

Shalaka Dewan,[a] Johanan H. Odhner,[a] Katharine Moore Tibbetts,[b] Sepideh Afsari,[a] Robert J. Levis[a] and Eric Borguet*[a]

Received 2nd June 2016,
Accepted 17th June 2016

DOI: 10.1039/c6tc02283a

www.rsc.org/MaterialsC

Photoluminescence from alkyl-capped silicon nanoparticles (Si NPs) synthesized by laser ablation of silicon in 1-octene is found to originate from two distinct species: narrowband UV-emitting alkyl-capped Si NPs and broadly tuneable (350–500 nm) emission associated with a solvent by-product. Our results demonstrate the need to effectively separate solvent by-products, a step which is often overlooked in ablation studies, before characterizing the optical properties of ablation-synthesized NPs for luminescence applications.

Introduction

Luminescent semiconductor nanoparticles are highly desirable due to their use in bio-imaging,[1] light emitting diode technology,[2] and other optoelectronic devices.[3] Substantial research has been undertaken to develop efficient syntheses of Si nanoparticles (NPs) with tailored optical properties.[4–7] While a wide variety of synthetic approaches have been devised for making Si NPs that emit strongly across the visible spectrum, the origin of the photoluminescence (PL) is not well understood.[8–10] Complicating matters, it has been shown that presence of impurities can change the PL of the Si NPs from the red region to the blue region of the spectrum.[11]

Alkyl-capped Si NPs generating strong UV-blue emission have been synthesized by a variety of methods, including mechano-photochemical treatment, microemulsion synthesis, chemical synthesis, and laser ablation.[12–15] Laser ablation synthesis of Si NPs using both nanosecond and femtosecond pulses offers an easy and efficient method of generating luminescent Si NPs.[16–19] An advantage of using laser ablation as a means for nanoparticle synthesis over traditional routes is the independence from chemical precursors (such as metal–organic substances), and the need for the addition of stabilizing ligands.[20] In addition, the possibility of tuning laser parameters to control the physical properties of the generated products provides an attractive route for developing tailor-made nanomaterials.[18] With this motivation, the generation of luminescent NPs in a one-pot synthesis by pulsed laser ablation in liquid has attracted significant interest. For instance, ablation of a Si wafer in neat 1-octene results in blue luminescent Si NPs covered in a monolayer of *n*-alkyl chains as a result of the reaction between the Si surface radicals and the 1-octene.[5,21]

The PL exhibited by Si NPs synthesized by laser ablation is typically broader than that of chemically synthesized Si NPs.[5,17,22,23] Broad PL spectra in Si NP preparations have, in general, been attributed to a broad NP size distribution.[9,24] This has spurred efforts towards controlling the size distribution of target nanoparticles by optimizing laser parameters and solvent conditions.[25,26] While most studies do not investigate the luminescence generated by solvent product,[5,16,18,23] a recent study reported that the luminescence of laser generated Si NPs are a 'perfect match' with the luminescence of the product formed by irradiation of the solvent alone.[27] The authors concluded that luminescence from the colloidal products arise from the graphitic carbon–polymer composite and not the generated Si-NPs.[27]

Here, we report the synthesis of UV-emitting Si NPs generated by the ablation of a Si target immersed in 1-octene by shaped femtosecond laser pulses. The PL of the ablation products is shown to arise from a combination of emission from two species: narrow emission from alkyl-capped Si NPs centred at 335 nm and broad emission between 350–500 nm from the irradiated solvent. The narrow UV-emitting Si NPs can be effectively separated from the carbon by-product. The PL of the solvent by-product shifts with increasing excitation wavelength, while the emission from the alkyl-capped Si NPs does not shift with excitation wavelength.

Experimental

Luminescent alkyl-capped Si NPs were synthesized by single-step laser ablation of a Si(111) wafer target using simultaneously

[a] Department of Chemistry and Center for Advanced Photonics Research, Temple University, Philadelphia, PA 19122, USA. E-mail: eborguet@temple.edu
[b] Department of Chemistry, Virginia Commonwealth University, Richmond, VA 23284, USA

† Electronic supplementary information (ESI) available: Experimental details, additional spectroscopic data, TEM images, and luminescence studies. See DOI: 10.1039/c6tc02283a

spatially and temporally focused (SSTF)[28,29] femtosecond pulses generated using a homebuilt apparatus (details in ESI†). In brief, 35 fs, 100 μJ laser pulses centred at 790 nm generated by a titanium–sapphire-based chirped-pulse amplifier laser were first shaped using SSTF and then focused onto the surface of a piranha cleaned Si(111) wafer immersed in neat 1-octene solvent through a quartz cuvette. The cuvette was mounted on a computer-controlled stage and translated vertically at a speed of 2 mm per second during irradiation so that each surface spot was irradiated by ~10 laser pulses (the beam waist is 20 μm). Since the irradiation time did not change the optical properties of the resulting Si NPs (see Fig. S2, ESI†), the products analysed in this discussion were irradiated for 80 seconds.

Post-processing of NPs

After ablation, the solvent was evaporated from the ablation products using a vacuum rotovap, followed by pumping for 18 h at <0.01 Torr pressure. The resulting (solid) residue was then dispersed in dichloromethane (DCM) and sonicated for 30 minutes. The sample prepared in this manner will be referred to as the "as-ablated sample". For the separation of carbon by-product, the sample solution after ablation was centrifuged ($18\,220 \times g$) for 90 minutes, whereupon the supernatant solution was collected and then subjected to evaporation as described above and re-dispersed in DCM. The portion of the sample recovered from the supernatant will be referred to as the "carbon by-product". The solid collected after centrifugation was separately treated in the same manner described for the supernatant and will be referred to as the "separated Si NPs".

Analysis of NPs

PL measurements were performed using dilute solutions (0.15 OD at absorbance peak 266 nm for the as-ablated and the separated Si NPs) of the samples dispersed in DCM inside 10 mm rectangular quartz cuvettes in a PTI Luminescence Spectrometer using a right-angle geometry. Peak maxima reported in electron-volts (eV) are evaluated after transforming the measured spectra into energy space, where a λ^2 intensity correction is made to account for the linear wavelength dispersion of the spectrograph.[30] The shifts in the positions of the 2nd order diffraction peaks of the excitation photons are a calibration offset. The infrared spectrum of the separated Si NPs was obtained at room temperature from a sample prepared by dropping the DCM-dispersed colloid on to a NaCl plate and allowing the solvent to evaporate. The spectrum was collected on a Bruker Tensor 27 FTIR spectrometer. Raman measurements were performed using a LabRAM HR Evolution microscope (Horiba) with a 532 nm excitation laser. The Raman samples were drop cast on clean quartz wafers. Transmission Electron Microscopy (TEM) images were recorded on a JEOL JEM-1400 TEM operating at an accelerating voltage of 120 kV. A few drops of the solution of particles dispersed in DCM were drop cast on an ultrathin carbon type-A 400 mesh copper grid or Substratek™, 10–20 nm TiO_x on 300 mesh Cu grid (Ted Pella Inc., Redding, CA) Energy-dispersive X-ray spectroscopy (EDS) was performed on the TEM samples for elemental detection.

Results and discussion

The as-ablated sample shows strong blue PL under a handheld UV lamp (~340 nm) (Fig. 1a inset). The corresponding PL spectra cover the range of 300–500 nm (Fig. 1a). The emission red-shifts as the excitation wavelength is tuned from 260 to 400 nm (Fig. 1a), consistent with previous reports on Si NPs generated by laser ablation.[5,17,22] The PL spectra have peak widths of ~100 nm (FWHM) over the whole range. The peak emission intensity is observed at ~330 nm (3.75 eV) with 280 nm (4.43 eV) excitation, in agreement with results obtained for chemically synthesized heptyl-capped Si NPs.[31] However, this PL is broader than that of chemically synthesized alkyl-capped Si NPs,[31–33] an observation that has been attributed to a broad particle size distribution.[8] While most ablation studies do not discuss the influence of the laser irradiation of the solvent on the PL spectrum,[17,23] Intartaglia *et al.* reported that the PL of Si NPs produced by laser ablation was identical to the PL of the irradiated solvent alone.[27] The carbon by-product was observed as large, amorphous structures in

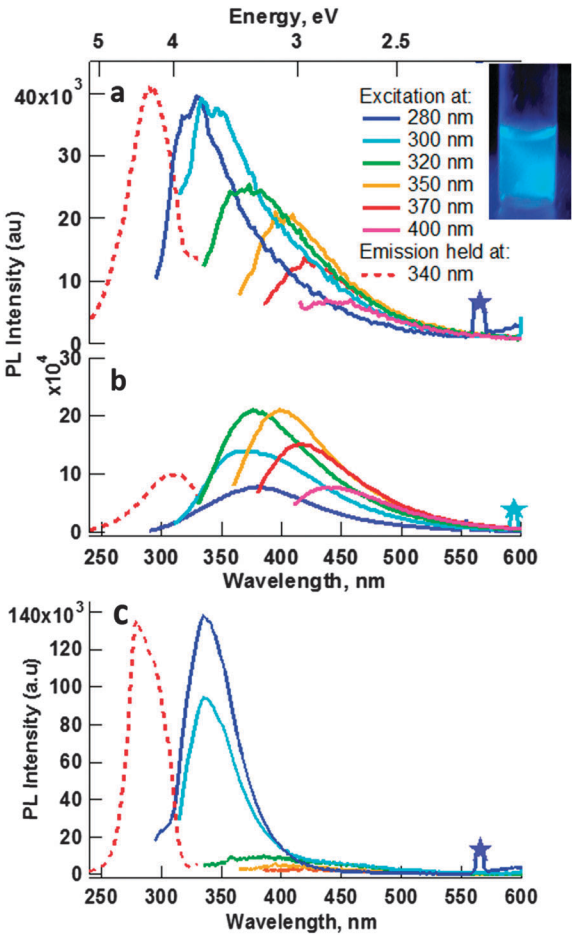

Fig. 1 PL from Si NPs generated by shaped femtosecond laser pulse ablation of Si in 1-octene. PL spectra (solid lines) and excitation scans (dotted lines) of (a) as-ablated sample before separation and (b) control sample (irradiation of neat 1-octene). (c) Si NPs after separation of carbon by-product. Inset: As-ablated sample under UV lamp illumination. Stars on the graphs indicate scattered 2nd order diffraction of the excitation photons.

TEM images.[27] The authors concluded that this carbon by-product, arising from the interaction of the pulsed laser with the solvent, accounted for the majority of the emission generated by the products of pulsed laser ablation of Si in toluene under the conditions reported.[27] Similar amorphous carbon structures were observed in our TEM images of the as-ablated products (Fig. S3, ESI†).

To determine the influence of the solvent on the observed PL of the as-ablated sample, 1-octene was irradiated under the same conditions as above but without the Si target. The products of solvent irradiation luminesced between 350–500 nm, and the spectrum was observed to red-shift as the excitation wavelength (Fig. 1b) was tuned to wavelengths >300 nm. However, contrary to the previous study by Intartaglia *et al.*, the PL of this control was different from that of the as-ablated sample, showing no intensity <350 nm. In our as-ablated samples, the difference between Si NP PL and that of solvent irradiation control is quite obvious (Fig. 1a and b), possibly because of the differences in the laser source used here (for *e.g.*, different wavelength and pulse width).

The similar emission profiles (Fig. 1a and b) at excitation wavelengths above 300 nm suggest that the luminescent product of 1-octene irradiation may also be generated in the ablation synthesis of Si NPs in the presence of 1-octene. The PL of the irradiated solvent is similar to that observed from carbon and graphene quantum dots, as well as from toluene irradiation.[34–36] Moreover, the excitation spectra of the as-ablated sample recorded for emission at 340 nm are blue-shifted with respect to the control (peaking at 290 nm as opposed to 310 nm, Fig. 1a and b). These findings suggest that the Si NPs generated by laser ablation have optical properties that are different from those of the carbon by-product and it may be possible to resolve them.

With this objective in mind, the separation of the carbon and silicon irradiation products was performed by centrifugation The PL spectrum of the alkyl-capped Si NPs after separation of the carbon by-product (Fig. 1c) is significantly different from the as-ablated Si NPs (Fig. 1a); moreover, the fluorescence is also narrower than that previously reported for laser ablated, alkyl-capped Si NPs.[17,23,37,38] The PL of the separated Si NPs, centred at 335 nm (3.64 eV), is consistent with that of chemically synthesized alkyl-capped Si NPs,[8,31,33] where emission in the ~330–360 nm region was attributed to be a result of electron–hole recombination across the direct Γ point transition in silicon (3.4 eV).[10,39] The blue-shift to 3.64 eV from 3.4 eV was said to be a result of quantum confinement.[39] The emission spectrum does not red-shift with increasing excitation wavelength, but only changes in amplitude, indicating that the PL likely originates from a direct band gap transition.[5] Low intensity PL observed in the separated Si NPs between 350 nm and 500 nm, for excitation at wavelengths >350 nm, is attributed to residual carbon by-product not removed in the centrifugation step. Since only one size distribution was synthesized in the experiments reported here, it was not possible to measure the effect of particle size on the PL spectrum and no definitive conclusions about the role of quantum confinement can be made. We note that the PL spectrum of the separated Si NPs was the same for all laser energies used during ablation (Fig. S4, ESI†).

The PL spectra of the separated carbon by-product (Fig. S5, ESI†) are very similar to those of the irradiated 1-octene control, suggesting that the origin of the broad, tuneable emission in the as-ablated sample is a result of a carbon by-product generated in the solvent and is unrelated to the size of the Si nanoparticles. The contribution of the laser ablation by-product to the PL of Si NPs is an important consideration in the application of pulsed-laser ablation as the synthetic route for optical nanostructures. These observations highlight the need to separate the target material from undesirable by-products.

The successful separation of the carbon by-product from the Si NPs was verified by individually analysing the isolated products by EDS on selected TEM images. EDS mapping revealed a high concentration of silicon (Fig. 2a(ii)), coincident with the particles (Fig. 2a(i)), in the separated Si NP sample. The uniform distribution of carbon (Fig. 2a(iv)) in the separated Si NP sample originates from

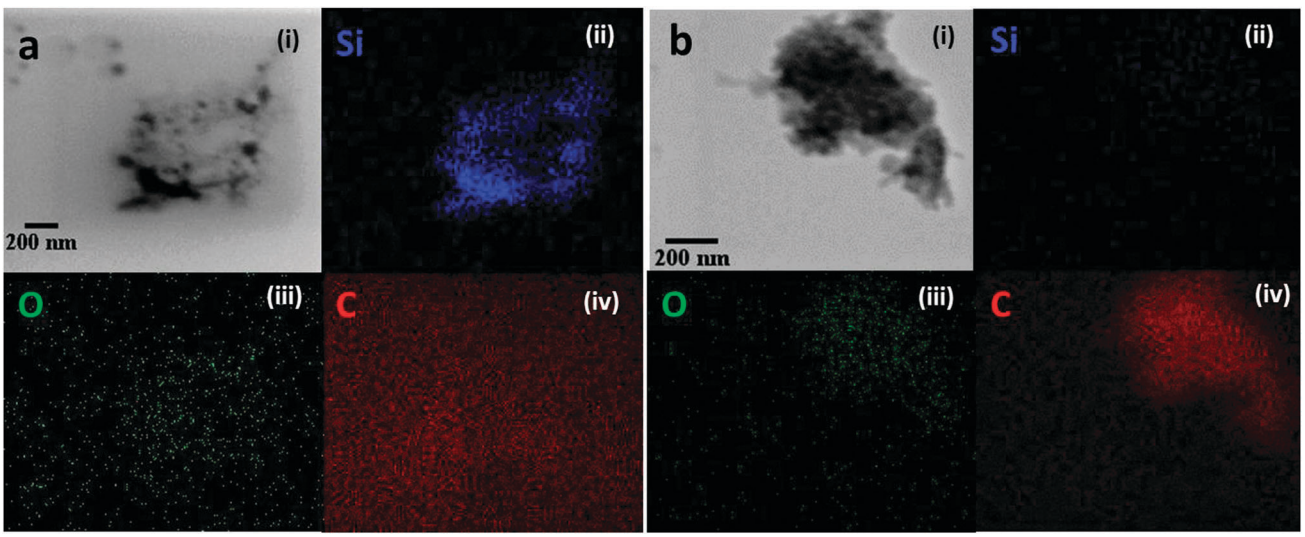

Fig. 2 EDS maps of TEM image of separated Si NPs: TEM images (i) of (a) separated Si NPs and (b) separated carbon by-product, along with the corresponding EDS map showing intensity for (ii) Si K alpha line, (iii) oxygen K alpha line, and (iv) carbon K alpha line.

the grid itself and confirms the effective separation of Si NPs from the solvent derived carbon product. On the other hand, no silicon K alpha emission is observed in the carbon by-product (Fig. 2b(ii)), but there are clearly carbon particles on the grid that can be distinguished from the background from the carbon grid itself (Fig. 2b(iv)). Low concentrations of oxygen are detected on both grids (Fig. 2a and b(iii)). Representative TEM images (Fig. 3) of the separated Si NPs show areas containing very small (<2 nm) particles (Fig. 3a) as well as areas containing larger ~5–10 nm particles (Fig. 3b and c), with an average diameter of 3.4 nm (Fig. 3d) for a sample of 260 objects.

To confirm that the separated Si NPs are capped by a monolayer of alkyl groups, IR and Raman spectroscopy were performed (Fig. 4a, b and Fig. S7, ESI†). The IR spectrum shows peaks at 2850 and 2920 cm^{-1} (Fig. 4a) corresponding to the aliphatic CH stretching modes of CH_2 and CH_3, suggesting the presence of a 1-octyl monolayer on the Si particles.[8] The bands at 1460 cm^{-1} and 1377 cm^{-1} have been observed before for alkyl-capped Si NPs and were assigned to the scissor vibration of Si–CH_2 or CH_3 deformation and the symmetric bending of CH_3, respectively (Fig. 4a).[8,31,33] There is no evidence for the presence of Si–O–C groups due to the absence of bands around 1070–1100 cm^{-1}.[40] Further confirmation of the presence of alkyl groups directly bound to Si is provided by the observation of a band at 1249 cm^{-1} corresponding to the symmetric bending of Si–C in Si–CH_2.[33] The Raman spectra of the separated Si NPs show a Si phonon peak at 500.3 cm^{-1} (Fig. 4b), red-shifted from the bulk Si crystal due to small particle size.[41] The magnitude of the Si Raman phonon red-shift corresponds to a particle size of <2 nm according to a recent 3D model, smaller than the average size determined from our TEM results (Fig. 3).[41] It is possible that particles of size <2 nm were undercounted in our size analysis due to low TEM resolution. Some variability in the Raman peak position of the Si phonon

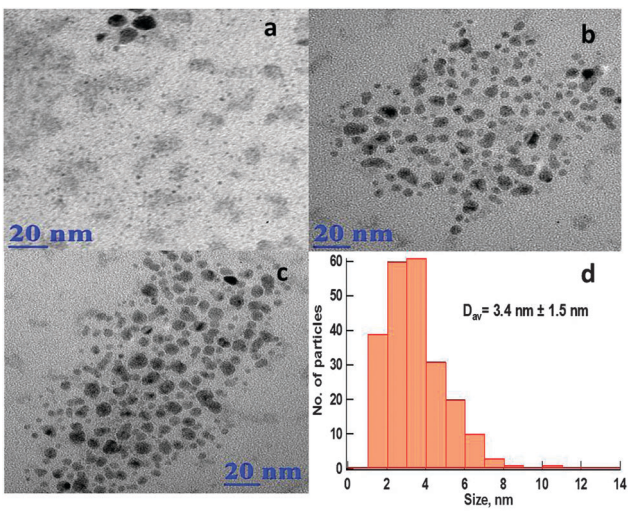

Fig. 3 TEM images and particle size analysis of the separated Si NPs. (a–c) TEM images of the sample at different areas of the TEM grid and (d) result of the size distribution analysis performed using 260 particles over three TEM images.

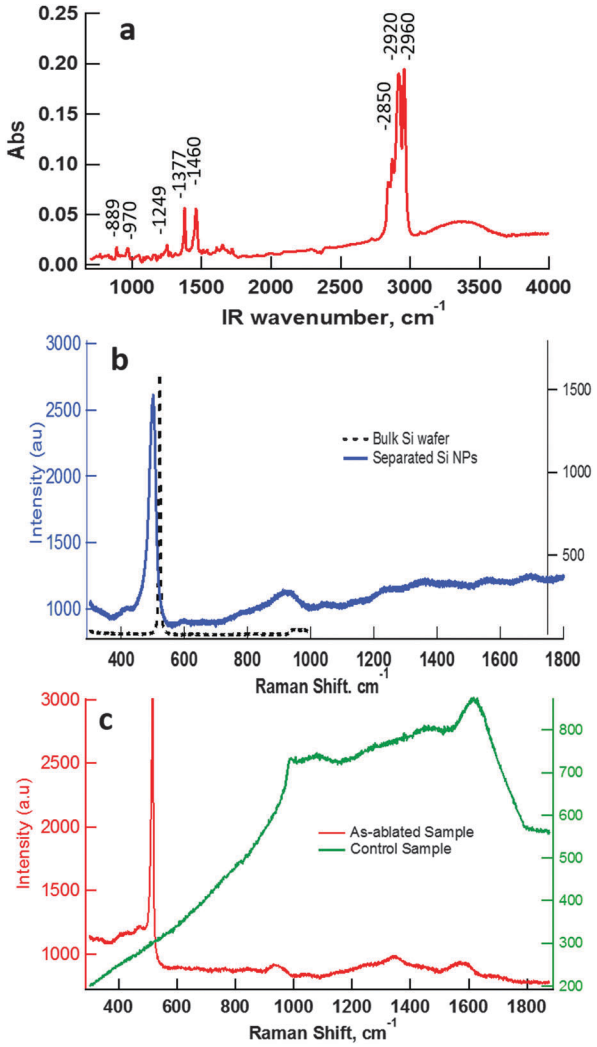

Fig. 4 Spectroscopic analysis of separated Si NPs: (a) FTIR and (b) Raman spectra of the separated alkyl-capped Si NPs at 532 nm excitation and silicon bulk Raman band shown as a reference (c) Raman spectra of the as-ablated sample under 532 nm excitation and 1-octene irradiated control sample under 325 nm excitation.

(±6 cm^{-1}) was observed for samples prepared on different days. However, previous experimental studies have reported Raman shifts in the 510–500 cm^{-1} range for Si nanocrystals with comparable sizes to our samples (3.4 ± 1.5 nm).[42–44] The crystallinity of the Si NPs was verified by selected area electron diffraction (SAED) of the as-ablated samples, which showed distinct diffraction spots that are consistent with silicon crystal structure (Fig. S6, ESI†).

The Raman spectrum of the as-ablated sample also shows features around 1350 and 1575 cm^{-1} (Fig. 4c), corresponding to the D and G bands of graphitic carbon, respectively, in addition to the Si phonon peak at ~500 cm^{-1} (Fig. 4c).[45] The UV Raman spectrum (325 nm) of the irradiated 1-octene control sample exhibits features corresponding to the D, G, and T bands, which are significantly broadened, and is typical of amorphous carbon products.[46–49] The FTIR spectra of the irradiated 1-octene and the separated carbon by-product, on the other hand, did not

show any aromatic or aliphatic C–H stretch features, (Fig. S7a, ESI†), suggesting that the carbon by-product may also contain amorphous carbon. The determination of the exact composition of the carbon by-product will be the efforts of future studies.

Conclusions

We have demonstrated that the broad, tuneable photoluminescence reported for silicon nanoparticles synthesized by laser ablation in organic liquids originates from two different species that can be separated as: narrow-band, UV-emitting alkyl-capped Si NPs and a solvent irradiation carbon by-product whose emission is relatively broad and tuneable from 350–500 nm. Contrary to the findings of previous studies,[27,45] our results show that the PL of Si NPs is not only different from that generated by laser interaction with the solvent, but, once separated, the emission from alkyl-capped Si NPs, centred at 335 nm (3.64 eV), looks remarkably similar to the PL of chemically synthesized alkyl-capped Si NPs.[31] Our results show that luminescent carbon by-products formed during laser ablation in an organic solvent can be systematically removed from the Si NPs, revealing the UV emission of alkyl-capped SI NPs. This study highlights importance of separating reaction by-products before considering the optical properties of nanostructures produced by laser ablation in solvent.

Acknowledgements

Support of this research by the Army Research Laboratory through contract W911NF-10-2-009 is gratefully acknowledged. The authors acknowledge NSF instrumentation grant (CHE-0923077) for the JEOL JEM-1400 TEM used in this research. Authors thank the Sieburth Lab for assistance in sample processing. TEM grids were generously provided by Neretina Lab. SD thanks Gregory Fiorin for assistance with Raman experiments.

Notes and references

1 F. Erogbogbo, K. T. Yong, I. Roy, G. Xu, P. N. Prasad and M. T. Swihart, *ACS Nano*, 2008, **2**, 873–878.
2 F. Maier-Flaig, J. Rinck, M. Stephan, T. Bocksrocker, M. Bruns, C. Kubel, A. K. Powell, G. A. Ozin and U. Lemmer, *Nano Lett.*, 2013, **13**, 475–480.
3 V. Biju, T. Itoh, A. Anas, A. Sujith and M. Ishikawa, *Anal. Bioanal. Chem.*, 2008, **391**, 2469–2495.
4 T. M. Atkins, A. Y. Louie and S. M. Kauzlarich, *Nanotechnology*, 2012, **23**, 294006.
5 N. Shirahata, M. R. Linford, S. Furumi, L. Pei, Y. Sakka, R. J. Gates and M. C. Asplund, *Chem. Commun.*, 2009, 4684–4686.
6 N. Arul Dhas, C. P. Raj and A. Gedanken, *Chem. Mater.*, 1998, **10**, 3278–3281.
7 L. Mangolini, E. Thimsen and U. Kortshagen, *Nano Lett.*, 2005, **5**, 655–659.
8 N. Shirahata, T. Hasegawa, Y. Sakka and T. Tsuruoka, *Small*, 2010, **6**, 915–921.
9 J. P. Wilcoxon and G. A. Samara, *Appl. Phys. Lett.*, 1999, **74**, 3164–3166.
10 S. Yang, W. Li, B. Cao, H. Zeng and W. Cai, *J. Phys. Chem. C*, 2011, **115**, 21056–21062.
11 M. Dasog, Z. Yang, S. Regli, T. M. Atkins, A. Faramus, M. P. Singh, E. Muthuswamy, S. M. Kauzlarich, R. D. Tilley and J. G. C. Veinot, *ACS Nano*, 2013, **7**, 2676–2685.
12 D. S. English, L. E. Pell, Z. Yu, P. F. Barbara and B. A. Korgel, *Nano Lett.*, 2002, **2**, 681–685.
13 K. Kůsová, O. Cibulka, K. Dohnalová, I. Pelant, J. Valenta, A. Fučíková, K. Žídek, J. Lang, J. Englich, P. Matějka, P. Štěpánek and S. Bakardjieva, *ACS Nano*, 2010, **4**, 4495–4504.
14 N. Shirahata, D. Hirakawa and Y. Sakka, *Green Chem.*, 2010, **12**, 2139–2141.
15 J. R. Siekierzycka, M. Rosso-Vasic, H. Zuilhof and A. M. Brouwer, *J. Phys. Chem. C*, 2011, **115**, 20888–20895.
16 H. Zeng, X.-W. Du, S. C. Singh, S. A. Kulinich, S. Yang, J. He and W. Cai, *Adv. Funct. Mater.*, 2012, **22**, 1333–1353.
17 D. Tan, Z. Ma, B. Xu, Y. Dai, G. Ma, M. He, Z. Jin and J. Qiu, *Phys. Chem. Chem. Phys.*, 2011, **13**, 20255–20261.
18 S. Hamad, G. K. Podagatlapalli, V. S. Vendamani, S. V. S. Nageswara Rao, A. P. Pathak, S. P. Tewari and S. Venugopal Rao, *J. Phys. Chem. C*, 2014, **118**, 7139–7151.
19 S. Alkis, A. K. Okyay and B. Ortaç, *J. Phys. Chem. C*, 2012, **116**, 3432–3436.
20 S. Barcikowski and G. Compagnini, *Phys. Chem. Chem. Phys.*, 2013, **15**, 3022–3026.
21 V. Amendola and M. Meneghetti, *Phys. Chem. Chem. Phys.*, 2013, **15**, 3027–3046.
22 L. Wanbing, W. Liping, Y. Wei, W. Xinzhan, L. Xiaowei and F. Guangsheng, *Micro Nano Lett.*, 2012, **7**, 1125–1128.
23 K. Abderrafi, R. l. García Calzada, M. B. Gongalsky, I. Suárez, R. Abarques, V. S. Chirvony, V. Y. Timoshenko, R. Ibáñez and J. P. Martínez-Pastor, *J. Phys. Chem. C*, 2011, **115**, 5147–5151.
24 N. Shirahata, *Phys. Chem. Chem. Phys.*, 2011, **13**, 7284–7294.
25 L. Patrone, D. Nelson, V. Safarov, M. Sentis and W. Marine, *J. Lumin.*, 1998, **80**, 217–221.
26 P. G. Kuzmin, G. A. Shafeev, V. V. Bukin, S. V. Garnov, C. Farcau, R. Carles, B. Warot-Fontrose, V. Guieu and G. Viau, *J. Phys. Chem. C*, 2010, **114**, 15266–15273.
27 R. Intartaglia, K. Bagga, A. Genovese, A. Athanassiou, R. Cingolani, A. Diaspro and F. Brandi, *Phys. Chem. Chem. Phys.*, 2012, **14**, 15406–15411.
28 J. H. Odhner, K. M. Tibbetts, B. Tangeysh, B. B. Wayland and R. J. Levis, *J. Phys. Chem. C*, 2014, **118**, 23986–23995.
29 B. Tangeysh, K. Moore Tibbetts, J. H. Odhner, B. B. Wayland and R. J. Levis, *J. Phys. Chem. C*, 2013, **117**, 18719–18727.
30 J. Mooney and P. Kambhampati, *J. Phys. Chem. Lett.*, 2013, **4**, 3316–3318.
31 R. D. Tilley, J. H. Warner, K. Yamamoto, I. Matsui and H. Fujimori, *Chem. Commun.*, 2005, 1833–1835.
32 F. Hua, M. T. Swihart and E. Ruckenstein, *Langmuir*, 2005, **21**, 6054–6062.
33 C.-S. Yang, R. A. Bley, S. M. Kauzlarich, H. W. H. Lee and G. R. Delgado, *J. Am. Chem. Soc.*, 1999, **121**, 5191–5195.

34 S. Yang, H. Zeng, H. Zhao, H. Zhang and W. Cai, *J. Mater. Chem.*, 2011, **21**, 4432–4436.
35 Y. Dong, J. Shao, C. Chen, H. Li, R. Wang, Y. Chi, X. Lin and G. Chen, *Carbon*, 2012, **50**, 4738–4743.
36 H. Li, X. He, Z. Kang, H. Huang, Y. Liu, J. Liu, S. Lian, C. H. A. Tsang, X. Yang and S.-T. Lee, *Angew. Chem., Int. Ed.*, 2010, **49**, 4430–4434.
37 N. Mansour, A. Momeni, R. Karimzadeh and M. Amini, *Opt. Mater. Express*, 2012, **2**, 740–748.
38 J. Wang, S. Sun, F. Peng, L. Cao and L. Sun, *Chem. Commun.*, 2011, **47**, 4941–4943.
39 J. P. Wilcoxon, G. A. Samara and P. N. Provencio, *Phys. Rev. B: Condens. Matter Mater. Phys.*, 1999, **60**, 2704–2714.
40 K. A. Pettigrew, Q. Liu, P. P. Power and S. M. Kauzlarich, *Chem. Mater.*, 2003, **15**, 4005–4011.
41 G. Faraci, S. Gibilisco, A. R. Pennisi and C. Faraci, *J. Appl. Phys.*, 2011, **109**, 074311.
42 C. M. Hessel, J. Wei, D. Reid, H. Fujii, M. C. Downer and B. A. Korgel, *J. Phys. Chem. Lett.*, 2012, **3**, 1089–1093.
43 C. Meier, S. Lüttjohann, V. G. Kravets, H. Nienhaus, A. Lorke and H. Wiggers, *Phys. E*, 2006, **32**, 155–158.
44 H. Xia, Y. L. He, L. C. Wang, W. Zhang, X. N. Liu, X. K. Zhang, D. Feng and H. E. Jackson, *J. Appl. Phys.*, 1995, **78**, 6705–6708.
45 S. Hamad, G. Krishna Podagatlapalli, R. Mounika, S. V. S. Nageswara Rao, A. P. Pathak and S. Venugopal Rao, *AIP Adv.*, 2015, **5**, 127127.
46 A. C. Ferrari and J. Robertson, *Phys. Rev. B: Condens. Matter Mater. Phys.*, 2001, **64**, 075414.
47 S. Osswald, G. Yushin, V. Mochalin, S. O. Kucheyev and Y. Gogotsi, *J. Am. Chem. Soc.*, 2006, **128**, 11635–11642.
48 K. W. Gilkes, H. S. Sands, D. N. Batchelder, J. Robertson and W. I. Milne, *Appl. Phys. Lett.*, 1997, **70**(15), 1980–1982.
49 V. I. Merkulov, J. S. Lannin, C. H. Munro, S. A. Asher, V. S. Veerasamy and W. I. Milne, *Phys. Rev. Lett.*, 1997, **78**, 4869–4872.